SCIENTIFIC REPORTS

OPEN

SUBJECT AREAS:
APPLIED OPTICS
MATERIALS FOR OPTICS
NONLINEAR OPTICS
CHARACTERIZATION AND ANALYTICAL TECHNIQUES

Received
4 March 2013

Accepted
22 March 2013

Published
3 April 2013

Correspondence and requests for materials should be addressed to Z.P.W. (zpwang@sdu.edu.cn) or X.S. (sunxun@sdu.edu.cn)

Non-critical phase-matching fourth harmonic generation of a 1053-nm laser in an ADP crystal

Shaohua Ji[1], Fang Wang[2], Lili Zhu[1], Xinguang Xu[1], Zhengping Wang[1] & Xun Sun[1]

[1]State Key Laboratory of Crystal Materials, Shandong University, Ji'nan 250100, China, [2]Research Center of Laser Fusion, China Academy of Engineering Physics, Mianyang 621900, China.

In current inertial confinement fusion (ICF) facilities, KDP and DKDP crystals are the second harmonic generation (SHG) and third harmonic generation (THG) materials for the Nd:glass laser (1053 nm). Based on the trend for the development of short wavelengths for ICF driving lasers, technical solutions for fourth harmonic generation (FHG) will undoubtedly attract more and more attention. In this paper, the rapid growth of an ADP crystal and non-critical phase-matching (NCPM) FHG of a 1053-nm laser using an ADP crystal are reported. The NCPM temperature is 33.7°C. The conversion efficiency from 526 to 263 nm is 70%, and the angular acceptance range is 55.4 mrad; these results are superior to those for the DKDP crystals. This research has shown that ADP crystals will be a competitive candidate in future ICF facilities when the utilisation of high-energy, high-efficiency UV lasers at wavelengths shorter than the present 351 nm is of interest.

At present, the drivers in inertial confinement fusion (ICF) facilities are undoubtedly the most enormous and expensive laser systems on the Earth[1–4] and have been highly studied in recent years[5,6]. Because short wavelengths exhibit more efficient coupling with plasma and are favourable for the compression of pellets, the development of driver sources for ICF has always shifted from the near infrared towards the UV region. Currently, the third harmonic (351 nm) of Nd:glass is used as the working wavelength for many principal ICF projects, such as the National Ignition Facility (NIF) in the USA, the LMG Facility in France, and the SG Facility in China. The fourth harmonic (263 nm) of Nd:glass is anticipated to be a favourite candidate for the next generation of ICF equipment, and the proper nonlinear optical (NLO) material to perform this frequency conversion will be crucial. Presently, dihydrogen phosphate crystals are the only NLO material that can be used because of their excellent overall properties, especially the availability of large, metre-sized samples.

In all of the phase-matching (PM) configurations for nonlinear optical crystals, non-critical phase-matching (NCPM) along the $\Theta = 90^\circ$ direction is the most useful because this configuration has many advantages, including a large effective nonlinear optical coefficient (d_{eff}), a small PM angular sensitivity, no beam walk-off, and high utilisation of the as-grown crystal. Previously, NCPM fourth harmonic generation (FHG) of a 1053-nm Nd:glass laser and a 1064-nm Nd:YAG crystal laser were most concentrated in partially deuterated potassium dihydrogen phosphate (KD*P) crystals, i.e., $K(D_xH_{1-x})_2PO_4$ or DKDP, whose refractive index can be continuously adjusted by deuteration level or crystal temperature[7–10]. Compared with DKDP, the ammonium dihydrogen phosphate ($NH_4H_2PO_4$ or ADP) crystal has a larger NLO coefficient, a higher laser damage threshold, a shorter UV transmission cut-off, a faster growth speed and a much lower production cost. In 1977, angle-tuned, i. e., critical PM, FHG of a 1064-nm laser was performed with a traditionally grown ADP crystal[11]. To our knowledge, little progress on FHG with ADP crystals has been made since that time. In this paper, we introduce the rapid growth of a high-quality ADP crystal, the transmittance spectrum and thermal conductivity measurements of the ADP crystal, and a comparison of NCPM FHG experiments using ADP and DKDP crystals. The conversion efficiency, the output energy and the angular bandwidth of the ADP crystal were superior to those of the DKDP crystal. Based on comprehensive consideration of the crystal growth and NLO characteristics of ADP, we believe that ADP crystals will be a promising candidate for FHG in future ICF facilities and will be a powerful competitor against the DKDP and potassium dihydrogen phosphate (KDP) crystals that are extensively used today.

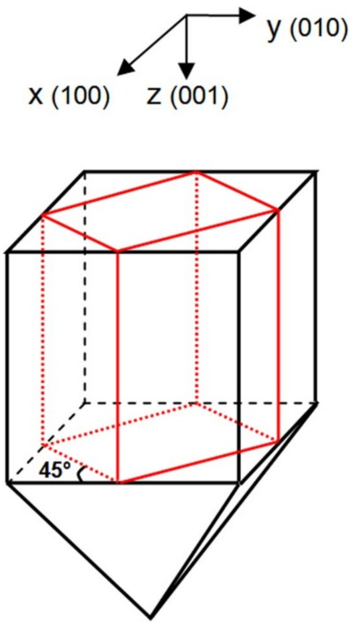

Figure 1 | Cutting schematic for the crystal samples.

Results

Sample preparation. Both the ADP and 74% D DKDP crystals were processed along the type-I NCPM direction, which was 90° relative to the z-axis ($\Theta = 90°$) and at 45° relative to the x-axis ($\Phi = 45°$), as shown in Fig. 1. The sizes of the experimental samples were 14.5 × 14.5 × 8.3 mm^3 for the ADP crystal and 14.5 × 14.5 × 9.1 mm^3 for the DKDP crystal. The transmittance faces of the crystals were polished but were not coated.

Experimental setup. The experimental setup for NCPM FHG is shown in Fig. 2. The fundamental light source A is a Nd:YLF laser at a wavelength of 1053 nm, with a pulse width of 50 ps, and a repetition rate of 1 Hz. The second harmonic generation (SHG) crystal C is KDP cut along the Type-I PM direction (41°, 45°), and the FHG crystal F is ADP or DKDP cut along the Type-I NCPM direction (90°, 45°). The ADP/DKDP sample is placed in a copper cube whose temperature is controlled with an accuracy of ±0.1°C. The copper cube is tightly sealed (one side is covered with optical glass and the other side is covered with quartz glass) to protect the ADP/DKDP sample from air circulation and the diffusion of heat. The FHG sample cube is mounted on an adjustable frame that can rotate around the $\Theta = 90°$ angle and can simultaneously maintain $\Phi = 45°$; in this way, the angular sensitivity of the crystal can be measured. The fundamental energy is monitored with the sampling system made of beam splitter B (PR @ 1053 nm) and energy calorimeter I. After SHG with crystal C, the remaining fundamental energy is completely reflected away from the optical path with beam splitter D (HR @ 1053 nm, HT @ 527 nm) and is absorbed by beam dump J. The SHG energy is detected with the sampling system made of beam splitter E (PR @ 527 nm) and energy calorimeter K. The generated FHG laser (263 nm) from crystal F is separated from the 527 nm laser with quartz prism G and is measured with energy calorimeter H.

Temperature tuning. For the ADP crystal, at a room temperature of 28°C, the exterior angle between the actual PM direction and the $\Theta = 90°$ direction was measured to be ~6°, and the corresponding internal angle was ~4°, based on the refractive index of the crystal. By slowly raising the crystal temperature to 33.7°C, the FHG PM angle was adjusted to the correct direction of $\Theta = 90°$, i.e., NCPM was realised at this condition. Fig. 3 shows the temperature tuning curve for ADP FHG near the NCPM temperature (TNCPM) of 33.7°C. The full-width at half-maximum (FWHM) temperature bandwidth was 0.7°C. Because the crystal length was 8.3 mm, the temperature bandwidth was determined to be 0.6°C·cm, and the temperature phase-mismatch sensitivity ($\partial\Delta\kappa/\Delta T$) was 9.3°$C^{-1}$·$cm^{-1}$. Similarly, the NCPM FHG temperature was measured to be 28.2°C for the 74% deuterated DKDP crystal. The corresponding temperature tuning curve is shown in Fig. 4. The FWHM temperature bandwidth was 1.6°C for the 9.1 mm long crystal; thus, the temperature bandwidth was 1.46°C·cm, and $\partial\Delta\kappa/\Delta T$ was 3.8°C^{-1}·cm^{-1}.

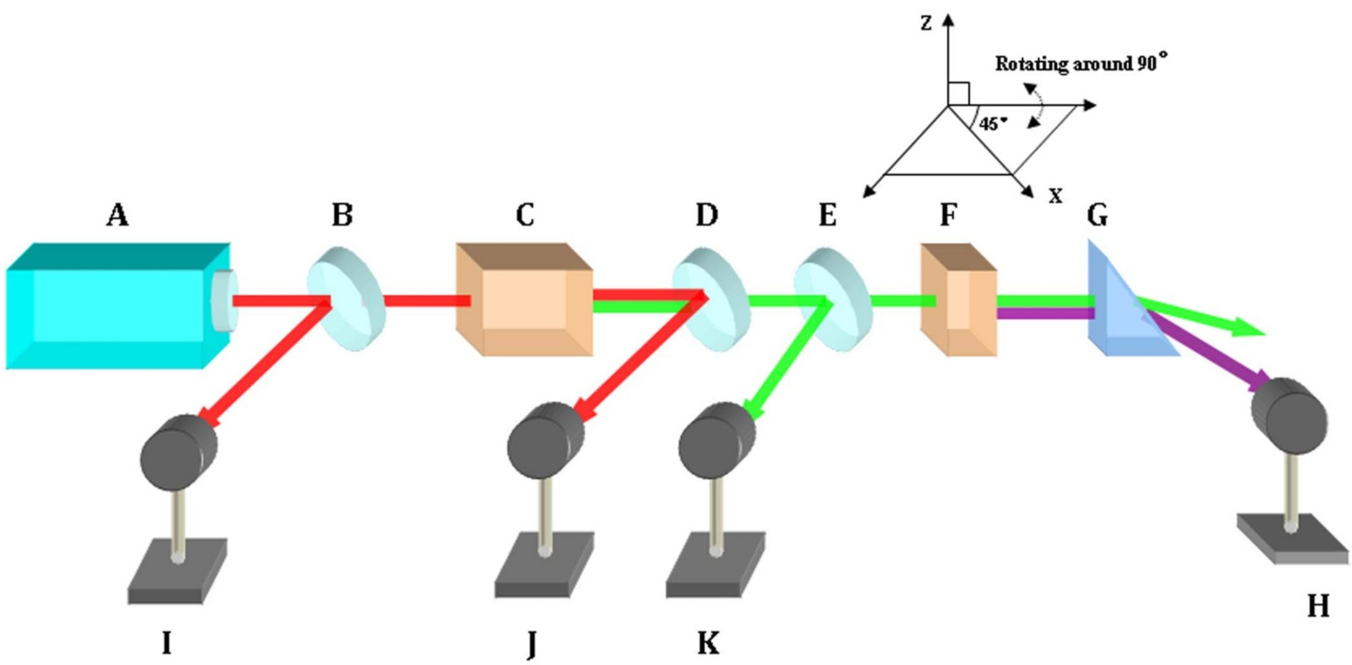

Figure 2 | Experimental setup for the NCPM FHG experiments. A. 1053-nm fundamental laser; B., D., E. beam splitters; C. SHG crystal; F. FHG crystal; G. quartz prism; H., I., K. energy calorimeters; and J. beam dump.

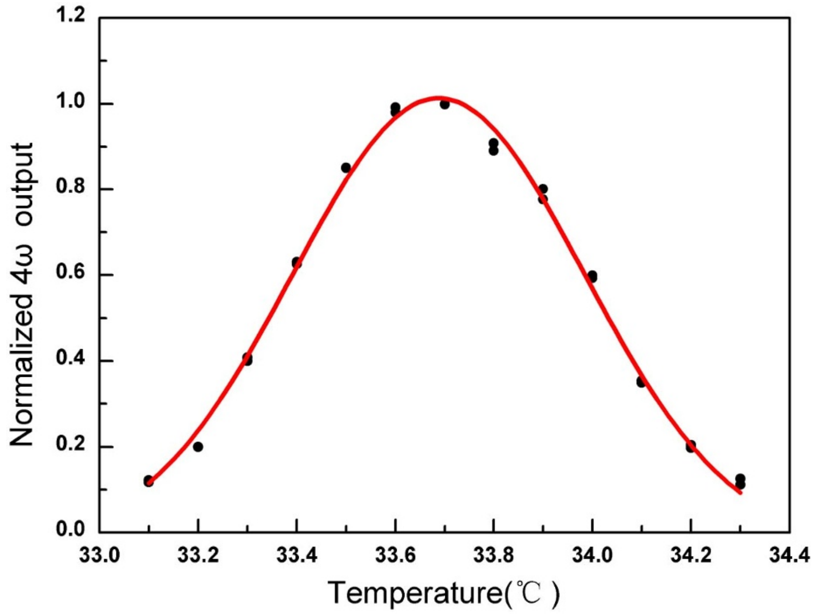

Figure 3 | Temperature tuning curve for NCPM FHG of laser radiation at 1053 nm for an ADP crystal.

Angle tuning. Maintaining the crystal temperature at the NCPM temperature, which was 33.7°C for the ADP crystal and 28.2°C for the DKDP crystal, we measured the angular sensitivity of the PM by monitoring the fourth harmonic output as the Θ angle of the crystal was rotated near the 90° angle. The results are shown in Fig. 5. The FWHM angular acceptance of ADP was 55.4 mrad, which was equivalent to an external angular acceptance of 50.5 mrad·cm$^{1/2}$ and an angular phase-mismatch sensitivity, $\partial^2\Delta\kappa/\Delta^2\Theta$, of 4.36 × 10^{-3} mrad^{-2}·cm^{-1}. Fig. 5 shows that the angular tuning curve of the ADP crystal had two symmetric wave packets, which might be caused by temperature fluctuations or by the small discrepancy in the parallelism between the two transmittance faces. For the DKDP crystal, the FWHM angular acceptance was 40 mrad, which corresponds to an external angular acceptance of 38.2 mrad·cm$^{1/2}$ and a $\partial^2\Delta\kappa/\Delta^2\Theta$ of 7. 62 × 10^{-3} mrad^{-2}·cm^{-1}. We also examined the angular phase-mismatch sensitivity of the DKDP sample at the critical PM condition. We fixed the crystal temperature at 26°C and slowly adjusted the crystal direction, deviating from Θ = 90°, until critical FHG PM was realised. In this situation, the FWHM angular acceptance was measured to be 10 mrad, which was only 1/4 of the value for the NCPM condition.

Conversion efficiency. By adjusting the energy of the 2ω beam (526 nm), we measured the FHG conversion efficiency of the ADP and DKDP crystals fixed at their individual NCPM conditions. The maximum 2ω output energy from the doubler was 50 mJ in a 50-ps pulse that was flat in time. The external conversion efficiency from 526 to 263 nm was obtained by simultaneously monitoring the

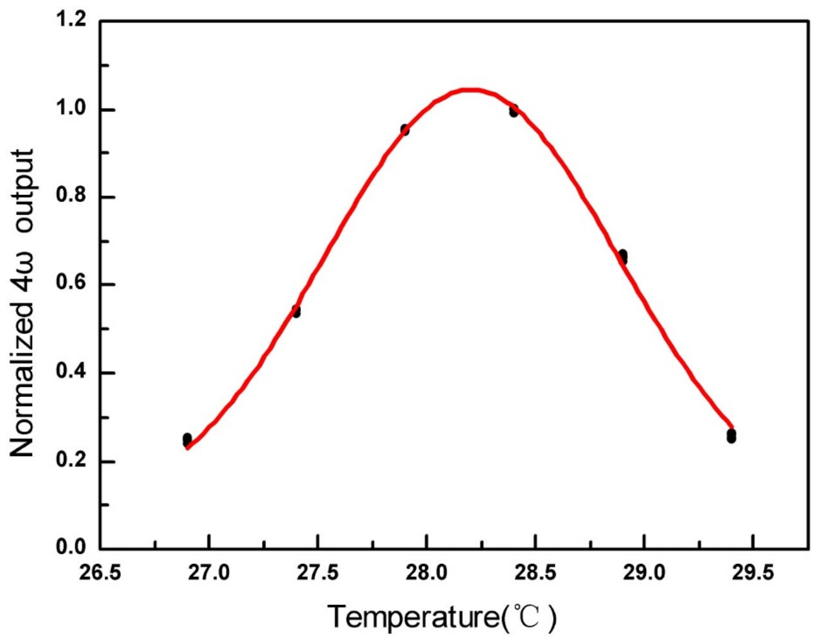

Figure 4 | Temperature tuning curve for NCPM FHG of laser radiation at 1053 nm for a 74%-deuterated DKDP crystal.

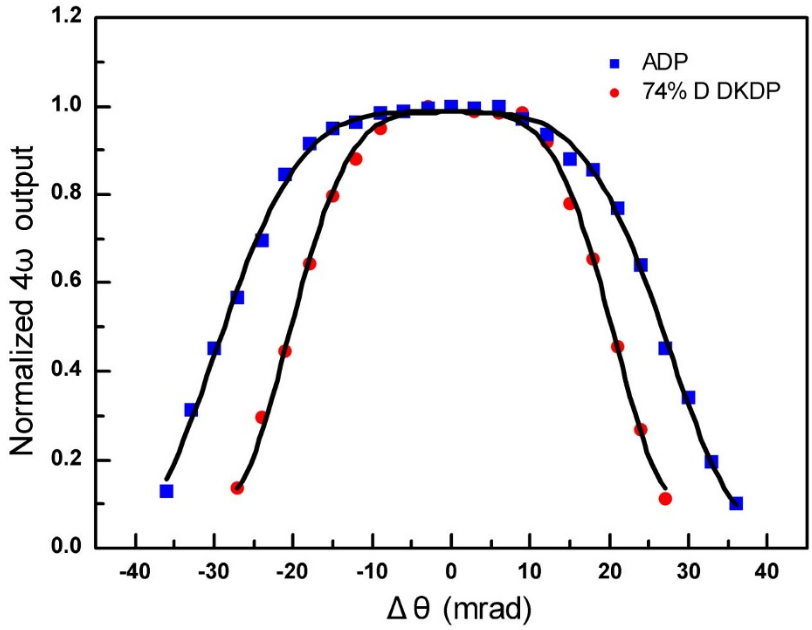

Figure 5 | External angular acceptance for NCPM FHG of 1053 nm radiation in ADP and DKDP crystals.

incident green pulses and the generated harmonic pulses, and the results are shown in Fig. 6. Over the entire range, the ADP crystal exhibited better conversion efficiency and a larger output energy than the DKDP crystal. For the ADP crystal, the highest conversion efficiency, 64.1%, appeared at the 2ω input energy of 28.7 mJ. Based on the Fresnel losses caused by the uncoated crystal surfaces and the losses of the quartz prism, the internal conversion efficiency was as high as 70% under these conditions. Above 30 mJ, as the 2ω input energy increased, the FHG conversion efficiency of ADP crystal slowly decreased. This problem arose because the crystal length did not match the large d_{eff} (0.57 pm/V) and could be solved by shortening the crystal to a more optimised length. For the DKDP crystal with similar length and smaller d_{eff} (0.46 pm/V), the FHG conversion efficiency did not obviously decrease until the 2ω input energy increased to the highest energy of 45.3 mJ. At this point, the maximum conversion efficiency and output energy of the DKDP crystal were 53.5% and 24 mJ, respectively.

Comprehensive evaluation. For several major tetragonal phosphates, which can be grown to the sizes required for ICF applications, the properties relevant to FHG of a 1053-nm Nd:glass laser are summarised in Table 1. The nonlinear parameters of KDP crystals, including the angular, temperature and wavelength acceptance, are shown for the critical PM condition at 30°C because to our knowledge, no NCPM FHG data of KDP have been revealed other than the NCPM temperature, i.e., 120°C[15], as listed in Table. 1. The

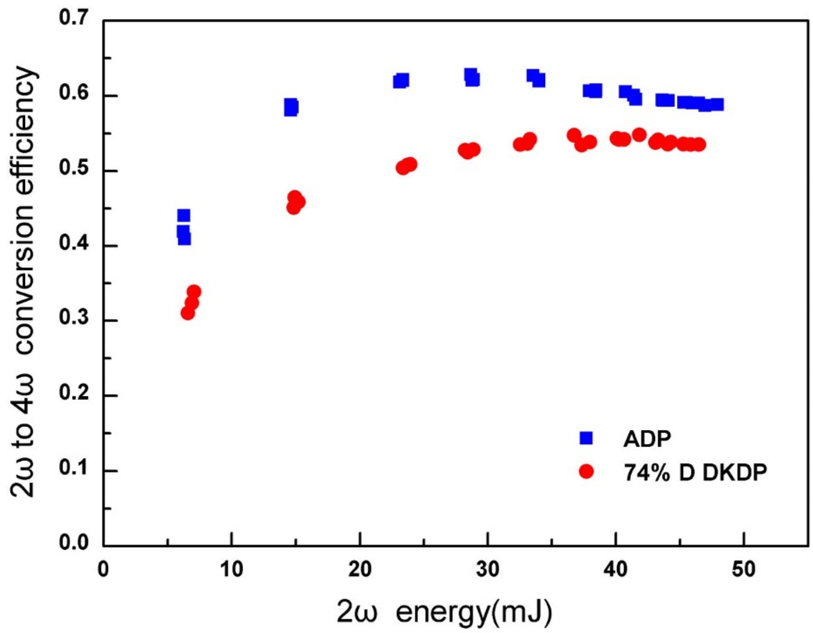

Figure 6 | External NCPM FHG conversion efficiency as a function of 2ω input energy.

Table 1 | Properties relevant to FHG of a 1053 nm Nd:glass laser for several large-sized phosphates

Crystal	KDP	DKDP	ADP
Transmission range (μm)[13]	0.174 ~ 1.57	0.2 ~ 2.1	0.18 ~ 1.53
Transmittance at 263 nm (μm) [a]	—	90.5% (traditional growth) 48.6% (rapid growth)	94.6% (rapid growth)
Thermal conductivity ($Wm^{-1}K^{-1}$)	1.21 (// c-axis) [13] 1.34 (⊥ c-axis)[13]	1.46 (// c-axis) [a] 1.77 (⊥ c-axis) [a]	0.52 (// c-axis) [a] 1.13 (⊥ c-axis) [a]
Specific heat ($Jg^{-1}K^{-1}$) [a]	0.94	0.99	1.19
Thermal expansion coefficients ($10^{-6}K^{-1}$)[14]	39.2 (// c-axis) 22 (⊥ c-axis)	44 (// c-axis) 19 (⊥ c-axis)	10.7 (// c-axis) 27.2 (⊥ c-axis)
d_{eff} (pm/V) [b]	0.62	0.42	0.76
Angular acceptance (m rad·cm$^{1/2}$)	2.1 [c]	38.2 [a]	50.5 [a]
Temperature acceptance (°C·cm)	2.17 [c]	1.46 [a]	0.6 [a]
Wavelength acceptance (nm·cm)	0.135 [c]	0.14 [d]	0.1214
NCPM temperature for FHG at 1053 nm (°C)	120[15]	28.2 [a]	33.7 [a]
Laser damage threshold ($10^{12}W/m^2$)[13,16]	15 ~ 18 @ 1.064 μm, 10 ns 90 @ 0.5265 μm, 0.6 ns	10 @ 1.064 μm, 10 ns >80 @ 0.532 μm, 0.6 ns >100 @ 0.266 μm, 0.03 ns	30 @ 1.064 μm, 10 ns >130 @ 0.53 μm, 0.5 ns >100 @ 0.266 μm, 0.03 ns
Linear absorption coefficient α (cm^{-1})	0.01–0.2 @ 0.25725 μm[15] 0.01 @ 0.5265 μm[13]	0.035 @ 0.266 μm[11] 0.004–0.005 @ 0.5321 μm[13]	0.035 @ 0.266 μm[11] 0.00005 @ 0.5145 μm[13]
Two-photon absorption coefficient β (cm/GW)	0.27 @ 266 nm[17]	0.02 @ 266 nm[11]	0.06 @ 266 nm[11] 0.24 @ 266 nm[17]
TSRS gain (cm/GW)[18,19]	0.31 @ 532 nm 0.65 @ 266 nm	0.15 @ 532 nm [e] 0.30 @ 266 nm [e]	0.3 @ 442 nm

[a]experimental data from present work.
[b]For λ = 1.064 μm[15].
[c]For critical Type-I PM FHG at (80°, 45°) at 30°C[14], the unit of angular acceptance for KDP is mrad·cm.
[d]Converted to λ = 0.526 μm[9].
[e]70% D.

nonlinear parameters of the DKDP and ADP crystals are from the present work and from the recent report by Lawrence Livermore National Laboratory (LLNL)[9].

Compared with the critical PM of KDP, room temperature NCPM of ADP and DKDP will be preferred because ADP and DKDP are stable, are easy to control, preserve raw crystals, possess a much larger angular acceptance (~20 times), and can utilise the second order nonlinear optical coefficient d_{36} completely.

For NCPM FHG, ADP has many advantages over DKDP, including a larger d_{eff} (1.8 times), a better angular acceptance (1.3 times), a higher laser damage threshold, a shorter UV transmission cut-off, a higher specific heat and less thermal expansion; thus, it is more favourable for ADP crystals to achieve a large output energy and a high conversion efficiency, which has been confirmed by the present work. The point-seed rapid growth method has been given close attention in ICF projects because this method can reduce the supply risk of the large aperture NLO components. Fig. 7 shows that the optical quality of rapidly grown ADP is at the same level as that of traditionally grown DKDP and is much better than that of rapidly grown DKDP. This is another important advantage of ADP crystals.

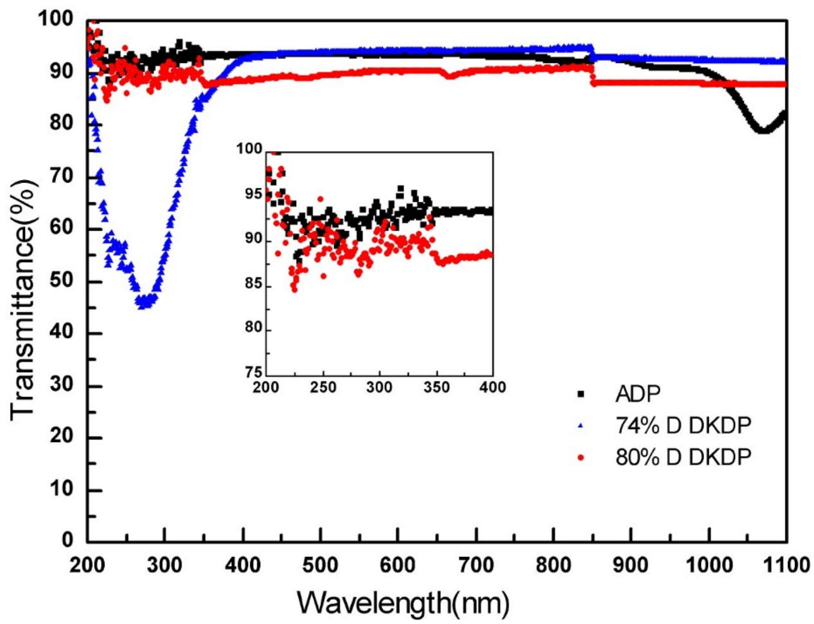

Figure 7 | Transmittance spectra of ADP and DKDP crystals grown through different methods.

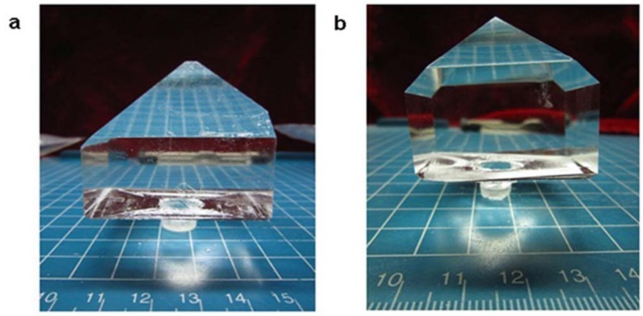

Figure 8 | Crystals grown by point-seed rapid-growth method. (a) ADP, (b) 74% DKDP.

The wavelength acceptances, NCPM temperatures and linear absorption coefficients of the DKDP and ADP crystals are comparable.

The disadvantages of ADP include a lower thermal conductivity, a narrower temperature acceptance, a larger two-photon absorption (TPA) coefficient and larger transverse-stimulated Raman scattering (TSRS) gain. For ADP crystals, the effects of these properties in high-energy, large-aperture NCPM FHG processes must be examined through more experiments in the future. Nevertheless, we are confident that these disadvantages can be ameliorated through technical improvements, such as optimising the operating frequency to minimise the low thermal conductivity, precise control of the crystal temperature to ameliorate the small temperature acceptance, adjustment of the experimental parameters against TPA, and

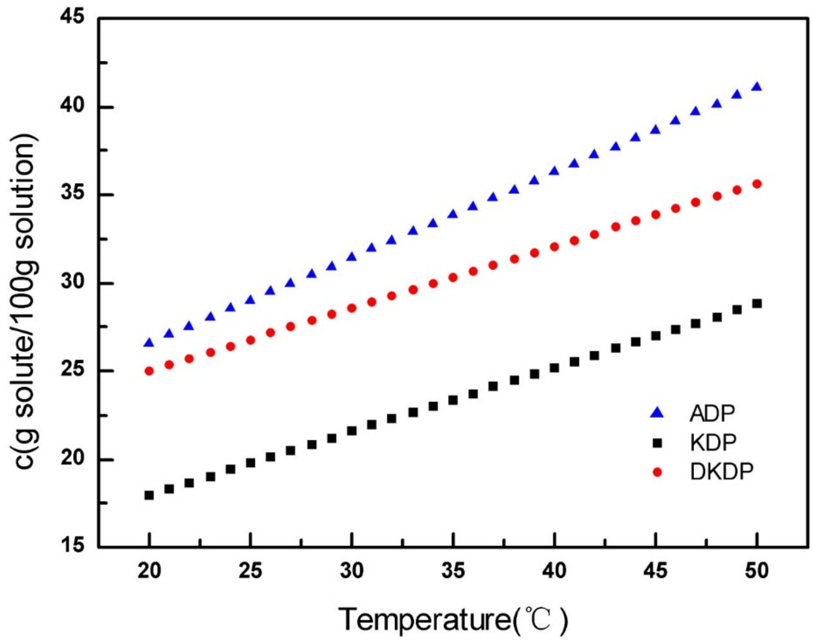

Figure 9 | Solubility curves for ADP/KDP/DKDP crystals over the temperature range from 20 to 50°C.

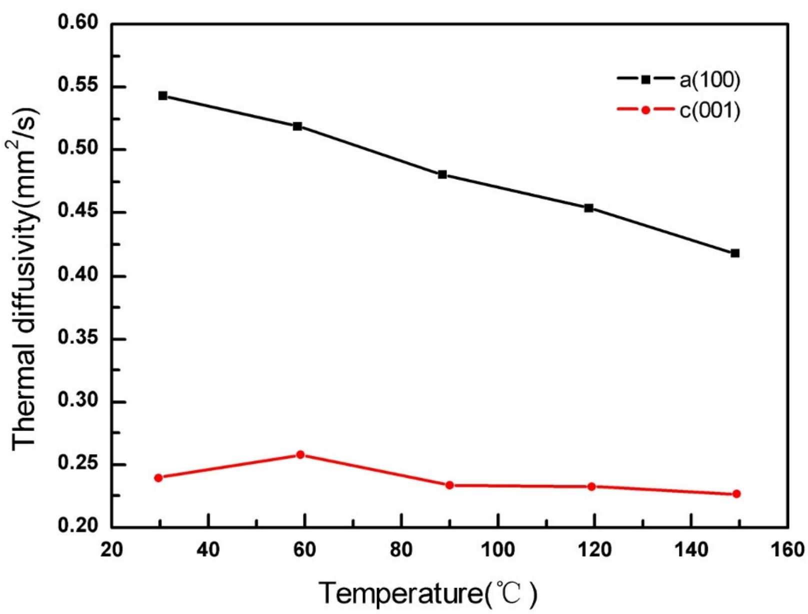

Figure 10 | Thermal diffusivity of ADP crystal.

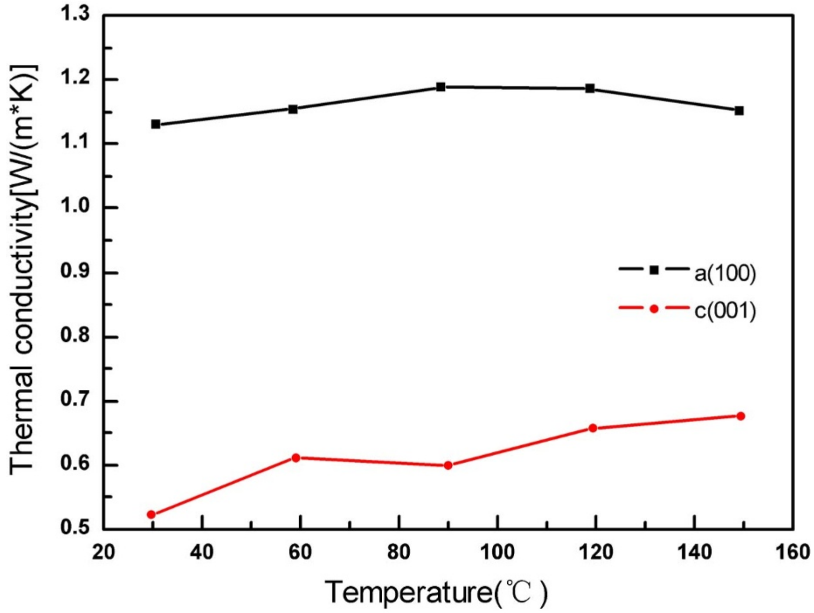

Figure 11 | Thermal conductivity of ADP crystal.

moderately changing the composition to prevent TSRS. It has been shown that deuterated KDP crystals can effectively decrease the TSRS gain compared with normal KDP crystals[18,20]; a similar phenomenon was found in a comparison of deuterated ammonium dihydrogen phosphate (DADP) and ADP crystals[19]; the partial-doping method can also be applied to ADP crystals to lessen the TSRS. In fact, in current ICF facilities, the edges and corners of large aperture NLO crystal components have compound chamfers and bevels to avoid multiple passes of side-scattered light; this technique is effective for the decrease of TSRS.

Discussion

Through the point-seeded rapid-growth method, high-quality ADP and DKDP crystals were grown. At a room temperature of 33.7°C, we obtained NCPM FHG of a 1053-nm laser in an ADP crystal for the first time. Compared with a 74% deuterated DKDP crystal, the ADP crystal exhibited a higher conversion efficiency, a larger output energy and a better angular acceptance. The highest efficiencies obtained for conversion from 526 to 263 nm were 70% for the ADP crystal and 58.2% for the DKDP crystal. The angular acceptance was measured to be 50.5 mrad·cm$^{1/2}$ for the ADP crystal and 38.2 mrad·cm$^{1/2}$ for the DKDP crystal. Although ADP crystals possess some drawbacks relative to DKDP crystals, including a low thermal conductivity, a narrow temperature acceptance, a larger TPA coefficient and TSRS gain, the attractive advantages of ADP, including the low cost, availability of large sizes at rapid growth speeds, large NLO coefficient, high laser damage threshold, broad angular acceptance, high specific heat and small thermal expansion

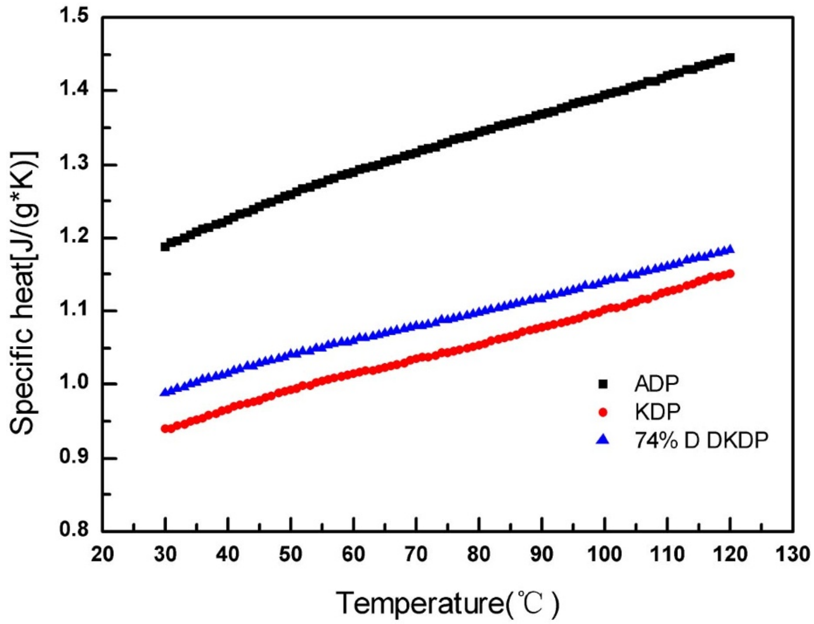

Figure 12 | Specific heats of ADP, KDP, and DKDP crystals.

Table 2 | Thermal conductivities of ADP and DKDP crystals at different temperatures

Temperature of ADP/K		303	333	363	393	423
Thermal conductivity of ADP/W/(m·K)	a (100)	1.13	1.15	1.19	1.19	1.15
	c (001)	0.52	0.53	0.60	0.66	0.68
Temperature of DKDP/K		295	338	357	397	412
Thermal conductivity of DKDP/W/(m·K)	a (100)	1.77	1.76	1.75	1.71	1.70
	c (001)	1.46	1.39	1.41	1.36	1.34

will make ADP one of the most preferred FHG materials in the construction of the next generation of ICF facilities or new UV subsystems for the present ICF facilities.

Methods

Crystal growth. The ADP crystal is grown through a point-seeded rapid growth method from a supersaturated solution, and the DKDP crystal was grown with the same method from aqueous solutions with a deuterium content of 80%. The deuterium content in the DKDP crystal is calculated to be 74% based on the reference method[12]. Crystallisation was performed in a temperature range from 45°C to 42°C. The velocity of the temperature reduction was maintained at 0.1°C/day. The crystal was rotated in the "forward-stop-backward" mode at a speed approximately 77 rpm. Photos of the crystal are shown in Figure 8 and reveal no visible macroscopic defects.

From the perspective of crystal growth, ADP is more soluble than KDP-type crystals, as shown in Fig. 9. Thus, more ADP can precipitate at a relatively small degree of supersaturation, and this effect gives ADP a higher growth rate. However, the dissolution of ADP is more difficult than that of KDP because the NH^{4+} will decrease the pH value of the solution. Thus, the growth of ADP is more difficult than that of KDP, and ADP may more easily develop occlusions and cracks. Growth with a conventional Z-cut seed is very difficult, and the process must be strictly controlled. Moreover, the ADP crystal is difficult to grow with a point-seed of KDP crystal because of the different parameters of the unit cells. In the experiment, we strictly control the supersaturation of the solution and finally obtain high-quality 100 mm crystals. The growth of larger ADP crystals is in progress.

Transmittance spectrum. For FHG, excellent UV transmittance is necessary and important. The transmittance spectra of the ADP and DKDP crystals are recorded with a model U-3500 spectrophotometer (HITACHI Inc., Japan). In Fig. 7, the ADP crystal is grown with the point-seed rapid-growth method, the 80%D DKDP(1) and 74%D DKDP(2) are grown with the traditional growth method and the point-seed rapid-growth method, respectively. Because crystal samples cut from different parts of a crystal will have differences in the UV transmittance, we ensure that all the samples are cut from the same position, are processed with identical techniques, and have identical transmission lengths. At the FHG wavelength of 263 nm, the transmittance of ADP is 94.6%, which is much higher than the 48.6% of DKDP(2) and is also slightly higher than the 90.5% of DKDP(1). This transmittance indicates that for FHG, the rapidly grown ADP is more favourable than the rapidly grown DKDP, and the absorption loss of rapidly grown ADP is at the same level as that of the traditionally grown DKDP.

Thermal conductivity. For large energies and high-efficiency frequency conversion, the thermal properties of a NLO material are an unavoidable topic. We examined the thermal diffusivity and thermal conductivity of ADP crystal with a laser thermal conductivity meter (LFA 457 MicroFlash, NETZSCH). The temperature range is 30 to 150°C (303 to 423 K), the heating interval is 30°C per step, and the results are shown in Fig. 10 and Fig. 11. For the thermal diffusivity, as the temperature increases, the (100) direction shows an obvious decrease, but the (001) direction is approximately constant. For the thermal conductivity, as the temperature increases, the (100) direction approaches a constant, and the (001) direction increases. In comparison, the measured thermal conductivities for both the ADP and DKDP crystals are listed in Table 2. The thermal conductivity of ADP is lower than that of DKDP; at a temperature of 300 K, the ratio is ~64% in the (100) direction and 36% in the (001) direction.

Specific heat. Specific heat is one of the most important thermal parameters. When a laser beam interacts with a NLO crystal, a certain amount of the incident energy is converted to thermal energy; this conversion leads to a temperature gradient inside the crystal. For a crystal with a large specific heat, the change in the thermal gradient of the crystal is small. These crystals might have large damage thresholds and can potentially be used in high energy laser systems. We measure the specific heat through differential scanning calorimetry with a simultaneous thermal analyser (METTLER-TOLEDO TGA/DSC/1600HT), and the results are shown in Fig. 12. At a temperature of 303 K, the specific heat of ADP is 1.19 $Jg^{-1}K^{-1}$, which is obviously superior to the 0.99 $Jg^{-1}K^{-1}$ of DKDP and the 0.94 $Jg^{-1}K^{-1}$ of KDP. This property is very favourable for application of ADP in the high pulse energy, intermittently operated ICF facilities.

1. Clery, D. Fusion power's road not yet taken. *Science* **334**, 445–448 (2011).
2. Clery, D. What's next for ICF? *Science* **324**, 328–329 (2009).
3. Jenkins, A. A new age for science. *Nature Photonics* **2**, 3–5 (2007).
4. Evens, R. Laser fusion: Hollow shells, shorter wavelengths. *Nature* **314**, 133–134 (1985).
5. Noorden, R. V., Ledford, H. & Mann, A. New year, new science. *Nature* **469**, 12 (2011).
6. Clery, D. NIF Report Asks for More Time to Achieve Ignition. *Science* **338**, 1519 (2012).
7. Bredikhin, V. I., Genkin, V. N., Kuznetsov, S. P. & Novikov, M. A. 90° phase-matching in $KD_{2x}H_{2(1-x)}PO4$ crystals upon doubling of the second harmonic of a Nd laser. *Sov. Tech. Phys. Lett.* **3**, 165–166 (1977).
8. Liu, Y. S., Jones, W. B. & Chernoch, J. P. High-efficiency high-power coherent UV generation at 266 nm in 90o phase-matched deuterated KDP. *Appl. Phys. Lett.* **29**, 32–34 (1976).
9. Yang, S. T. *et al.* Noncritically phased-matched fourth harmonic generation of Nd:glass lasers in partially deuterated KDP crystals. *Optics Letters* **36**, 1824–1826 (2011).
10. Ji, S. *et al.* Non-critical phasematching conditions for fourth harmonic generation of DKDP crystal. *Opt. Mater. Express* **2**, 735–739 (2012).
11. Reintjes, J. & Eckardt, R. C. Efficient harmonic generation from 532 to 266 nm in ADP and KD*P. *Appl. Phys. Lett.* **30**, 91–93 (1977).
12. Loiacono, G. M., Balascio, J. F. & Osborne, W. Effect of deuteration on the ferroelectric transition temperature and the distribution coefficient of deuterium in $K(H_{1-x}D_x)_2PO_4$. *Appl. Phys. Lett.* **24**, 455–456 (1974).
13. Dmitriev, V. G., Gurzadyan, G. G. & Nikogosyan, D. N. Handbook of nonlinear optical crystals. Berlin: *Springer*, 78–96 (1999).
14. Smith, A. V. SNLO nonlinear optics software: Version 58 nonlinear optics code, AS-Photonics, Albuquerque, NM.
15. Cleveland Crystals Catalog and their references. (www.clevelandcrystals.com/KDP.htm)
16. Li, G., Su, G., Zhuang, X., He, Y. & Li, Z. Growth of deuterated ammonium dehydrogen phosphate (DADP) crystal from solution and its characterization. *Journal of Synthetic Crystals* **33**, 192–196 (2004) Chinese.
17. Liu, P., Smith, W. L., Lotern, H., Bechtel, J. H. & Bloembergen, N. Absolute two-photon absorption coefficients at 355 and 266 nm. *Phys. Rev. B* **17**, 4620–4632 (1978).
18. Demos, S. G. *et al.* Measurement of the Raman scattering cross section of the breathing mode in KDP and DKDP crystals. *Optics Express* **19**, 21050–21059 (2011).
19. Gorelik, V. S. *et al.* Spontaneous Raman scattering spectra of ADP and DADP crystals in different polarization schemes. *Journal of Russian Laser Research* **29**, 357–363 (2008).
20. Barker, C. E. *et al.* Transverse stimulated Raman scattering in KDP. *Proc. SPIE* **2633**, 501–505 (1995).

Acknowledgements

This work is supported by the Natural Science Foundation of Shandong Province, China (ZR2010EM001), the Independent Innovation Foundation of Shandong University (IIFSDU, 2012JC016), the Program for New Century Excellent Talents in University (NCET-10-0552, NCET-10-0526), and the Natural Science Foundation for Distinguished Young Scholar of Shandong Province (JQ201218).

Author contributions

S.J. grew the crystals and prepared the samples, S.J., Z.W. and X.S. wrote the main text of the manuscript, S.J., F.W., L.Z. and X.X. prepared the experiments and contributed to the interpretation of the experimental data.

Additional information

Competing financial interests: The authors declare no competing financial interests.

How to cite this article: Ji, S. *et al.* Non-critical phase-matching fourth harmonic generation of a 1053-nm laser in an ADP crystal. *Sci. Rep.* **3**, 1605; DOI:10.1038/srep01605 (2013).